

1 Submitted to *Biogeosciences*

2
3 **Net primary production of Chinese fir plantation ecosystems**
4 **and its relationship to climate**

5
6 Ling Wang¹, Yuanbin Zhang², Frank Berninger^{2, 3}, Baoli Duan^{2, *}

7
8 ¹ Chengdu Institute of Biology, Chinese Academy of Sciences, PO Box 416, Chengdu 610041,
9 China

10 ² Key Laboratory of Mountain Surface Processes and Ecological Regulation, Institute of
11 Mountain Hazards and Environment, Chinese Academy of Sciences, Chengdu 610041, China

12 ³ Department of Forest Sciences, PO Box 27, FI-00014, University of Helsinki, Finland

13
14
15
16 * Correspondence address:

17 Baoli Duan (duanbl@imde.ac.cn)

18 Tel: 86-28-85554547

19
20
21 **Running title:** NPP of plantation ecosystem and climate

1 **Abstract** This article **investigates** the relationship between net primary production (NPP) of
2 Chinese fir, **temperature and precipitation**. The spatial-temporal NPP pattern in the potential
3 distribution area of Chinese fir from 2000 to 2010 was estimated utilizing **MODIS MOD17**
4 **product** in a Geographic Information System (GIS) environment. The results showed that **the**
5 **highest NPP value of Chinese fir is in the Fujian province in the eastern part of the study**
6 **region**. The relationship between NPP of Chinese fir and climate variables was analyzed
7 **spatially and temporally**. On the regional scale, precipitation showed higher correlation
8 coefficients with NPP than did temperature. The spatial variability pattern indicated that
9 temperature was more important in central and eastern regions (*e.g. Hunan and Fujian*
10 *province*), while precipitation was crucial in the northern part (*e.g. Anhui province*). Zonal
11 analysis revealed that the impact of precipitation on the production was more complicate than
12 that of temperature; **larger amount of precipitation is not always corresponding with greater**
13 **NPP value**. When compared to natural forests, plantations appear to be more sensitive to the
14 **variability** of precipitation, which indicates their higher vulnerability under climate change.
15 Temporally, NPP values decreased despite of increasing temperatures, and the decrease was
16 larger in plantations than among other vegetation types.

17

18

19 **Keywords:** NPP, Chinese fir plantation, Spatial-temporal pattern, Climate, GIS

20

21

22

1 **1. Introduction**

2

3 Chinese fir (*Cunninghamia lanceolata* (Lamb) Hook), a typical subtropical coniferous tree
4 species, is one of the most important timber species in Southern China due to its fast growth,
5 high yield and excellent wood quality (Wu, 1984). Traditionally, Chinese fir plantations were
6 established after native evergreen broad-leaved forests were harvested and slash-burned.
7 Since the 1950s, with the increasing demand for timber because of the economic development,
8 the plantation area of Chinese fir has been enlarged, and the species has been repeatedly
9 planted on the same sites without periods of fallow. Subsequently, decreasing production of
10 Chinese fir plantations has been reported since the 1980s (Fang, 1987; Ma, 2001), primarily
11 due to soil degradation (Ding *et al.*, 1999; Yang *et al.*, 2000). Climate influences the structure
12 and function of forest ecosystems and plays an essential role in the growth and health of forest.
13 Existing studies on the relationship between the productivity of plantations and climate are
14 scarce and limited to plot scale (Chen *et al.*, 1980 a & b; Lu, 1980). However, it is necessary
15 to clarify such relationships spatially at the regional level in order to extensively and
16 comprehensively understand the influence of climate on the productivity of plantations.
17 Moreover, climate change affects the growth and production of forests directly through
18 changes in the meteorological drivers of growth and through carbon dioxide fertilization, and
19 indirectly through complex interactions present in forest ecosystems. Temporal analyses of
20 such relationships are indispensable.

21

22 Forest ecosystems have the strongest carbon absorption capacities among all ecosystems. In

1 China, plantations are a significant part of forest ecosystems, and they are very important
2 when studying the carbon budget of terrestrial ecosystems. Since the early 1970s, the
3 plantation area of China has been gradually increasing to be now the highest in the world.
4 Forests in southern China are primarily plantations, which compose 54.3% of the total
5 plantation area of China. Carbon uptake by plantations is the most important reason for the
6 increased carbon storage in China (Fang *et al.*, 2001). It contributes about 65% of the C sink
7 in the terrestrial ecosystems of southern China (Wang *et al.*, 2009). Zhao (2010) showed that
8 the past decade (2000 to 2009) was the worldwide warmest one since instrumental
9 measurements of temperatures began in the 1880s. A better understanding of the decadal-scale
10 carbon balance dynamics of plantation ecosystems can benefit the interpretation of observed
11 variation in atmosphere-biosphere carbon exchanges (Fung *et al.*, 1997) and evaluation
12 policies to mitigate anthropogenic CO₂ emissions (IGBP Terrestrial Carbon Working Group
13 1998).

14
15 Net primary production (NPP) has received much attention not only because it is related to
16 the global carbon cycle but also because it is greatly influenced by the changing climate
17 (Prentice *et al.*, 2001). On the regional or global scale, NPP can be estimated by
18 process-based ecosystem models, which are based on the fundamental mechanisms
19 controlling NPP, such as moisture, temperature, solar radiation and nutrition (Running and
20 Coughlan, 1988; Melillo *et al.*, 1993). However, these ecosystem models generally estimate
21 potential NPP, primarily because of the difficulty in obtaining existing and detailed land cover
22 and soil information. On the other hand, satellite remote sensing data can provide near-real

1 time information regarding vegetation cover, biome type and disturbances (Wang *et al.*, 2013).
2 As a result, models using satellite data make NPP estimation simpler and possibly more
3 accurate (Potter *et al.*, 1993; Ruimy *et al.*, 1994; Field *et al.*, 1995; Zhao *et al.*, 2006).
4
5 Remote sensing has been used to monitor gross primary production (GPP) and NPP dynamics
6 on the regional and global scale (Nemani *et al.*, 2003; Zhao *et al.*, 2006). The Moderate
7 Resolution Imaging Spectroradiometer (MODIS) on NASA's satellites, Terra and Aqua, is one
8 of the most reliable data sources to monitor the terrestrial biosphere. The algorithm of MODIS
9 NPP is based on "radiation use efficiency", original logic proposed by Monteith (1972)
10 suggesting that NPP of well watered and fertilized annual crops is linearly related to the
11 amount of solar energy absorbed by the plants over a growing season. The resulting MODIS
12 GPP and NPP products have been validated as being able to capture spatial and temporal GPP
13 and NPP patterns across various biomes and climate regimes, and they are consistent with the
14 ground flux tower-based GPP and field-observed NPP estimation (Zhao *et al.*, 2005). The
15 availability of GPP and NPP calculated from the MODIS data provides a unique opportunity
16 for examining the spatial patterns of NPP in the plantation ecosystem of Chinese fir in
17 southern China and its relationships to climate. Consequently, the objectives of the current
18 study were to: (1) explore spatial-temporal patterns of NPP in the potential distribution area of
19 Chinese fir plantations; (2) examine the influence of temperature and precipitation on the
20 production of Chinese fir.

21

22

1 **2. Methods**

2

3 *2.1 Site description*

4

5 The study region chosen for this work is defined by the potential distribution area of Chinese
6 fir plantations, which spans a latitude range from 21.22 to 33.78 °N and longitude from 97.33
7 to 121.28 °E (Wu, 1984). It covers 10 provinces in southern China, including Zhejiang, Fujian,
8 Jiangxi, Hunan, Anhui, Guangdong, Guangxi, Yunnan, Sichuan and Chongqing, with a total
9 area of 134 million hectares (Fig. 1).

10

11 The potential distribution area of Chinese fir plantations is in the humid subtropical area in
12 southern China. This is a region of low mountains and hills with a very broken topography
13 and complicated geology. Plantations are generally located on slopes with steepness of more
14 than 20%, gentler lower slopes generally being used for agriculture. The soil type is usually
15 red earth, but the soil can be originated from very different parent materials. The soil
16 conditions vary significantly in terms of texture, depth, fertility, and other physical and
17 chemical characteristics. Naturally, Chinese fir is a component of mixed subtropical evergreen
18 broad-leaved forests (Wu, 1984).

19

20 *2.2 Data collection and processing*

21

22 Data sources required in the current study comprised MODIS NPP and GPP data, and land

1 cover and climate data. Remote sensing and geographic information system techniques were
2 employed for processing, analyzing and mapping of all spatial data. In addition, **R programming**
3 **language** (R Core Team, 2014), and a suite of R packages (sp (Bivand et al., 2013), rgdal
4 (Bivand et al., 2014), ggplot2 (Wickham, 2009)) was utilized for MODIS data download and
5 statistical analysis.

6

7 **MODIS data**

8

9 **MODIS product MOD 17 was chosen for evaluation of GPP and NPP in our study.** MODIS
10 data are formatted as a HDF EOS (Hierarchical Data Format - Earth Observing System) tile in
11 a sinusoidal projection with a grid of 1 km × 1 km. Each tile is 1200 × 1200 km (Zhao *et al.*,
12 2005). To cover the study area, six tiles with horizontal numbers from 26 to 28 and vertical
13 numbers from 5 to 6 for 11 years (2000-2010) were downloaded using the R script of
14 ModisDownload.R (<http://r-gis.net/?q=ModisDownload>). Six tiles of each time were merged
15 and converted into one GeoTIFF format image using MODIS Reprojection Tool (MRT). The
16 Sinusoidal projection of each image was transformed into an Albers Equal Area projection in
17 the process of converting HDF files into tiff images. The mosaic images were then clipped
18 into the study area in ESRI ArcInfo.

19

20 **Land cover data**

21

22 The 1-km resolution Landcover 2000 (GLC2000) data consistent geographically with the

1 study area was retrieved from the Global Landcover 2000 web site ([Bartholomé and Belward,](#)
2 [2005](#)). The GLC2000 data was based on the SPOT-4 vegetation VEGA2000 dataset, which
3 provides accurate baseline land cover information. Additionally, **the distribution of Chinese fir**
4 **was specially modified from the artificial Chinese forest map, which we applied from “Data**
5 **Sharing Network Infrastructure of Earth System Science” (<http://www.geodata.cn/>), a Chinese**
6 **web that provides data related to nature science. The distribution area of Chinese fir is**
7 **corresponding to that of coniferous forest partly in Global Landcover 2000. So we replaced those**
8 **coniferous forest areas with Chinese fir utilizing ArcGIS software to make a new land cover map**
9 **that contains Chinese fir.** The land cover data was then transformed to the same projection with
10 the MODIS data (Fig. 2).

11

12 **Climate data**

13

14 Average annual precipitation and temperature data (2000-2010) from **75** stations were
15 acquired as a text file from Chinese meteorological data sharing service system
16 (<http://cdc.cma.gov.cn>). The temperature and precipitation data were transformed into the grid
17 format from the text format in ArcInfo. To match MODIS data and land cover data, **ordinary**
18 **kriging was chosen as an estimator to interpolate the climatic data to be gridded surface with**
19 **resolution of 1 km using a module of the geostatistical analyst in ArcGIS.** A unified projection
20 corresponding to all other data was then defined for the interpolated temperature and
21 precipitation data. The trends of regional climatic variables in time series were analyzed based
22 on the Mann-Kendall method using R. The Mann-Kendall method is considered to be more

1 suitable for non-normally distributed data, which are frequently encountered in
2 hydro-meteorological time series (Yue *et al.*, 2002).

3

4 *2.3 Analysis of NPP temporal change pattern*

5

6 The temporal fluxes of NPP over the eleven study years were examined with the temporal
7 change tendency analysis for each pixel separately, utilizing the following equation:

$$8 \quad Q_{slope} = \frac{n \times \sum_{i=1}^n i \times NPP_i - (\sum_{i=1}^n i)(\sum_{i=1}^n NPP_i)}{n \times \sum_{i=1}^n i^2 - (\sum_{i=1}^n i)^2} \quad (1)$$

9 where n is the total number of study years and NPP_i is annual NPP during the year i of each
10 pixel (Stow *et al.*, 2003). Positive Q_{slope} signifies an increasing tendency through the time
11 series, while a negative one infers a decline. A higher absolute value of Q_{slope} denotes a
12 stronger magnitude of an increase or a decrease. The Q_{slope} parameter here was used as a
13 binary indicator to show whether NPP is increasing or decreasing at each pixel. Percentages
14 of pixels that decrease growth are presented in the results. Spatially, NPP patterns were
15 characterized by calculating the 11-year average NPP values geographically.

16

17 *2.4 Analysis between NPP pattern and climate variables*

18

19 To examine the relationship between the geographical NPP pattern and climatic factors, a
20 spatial correlation analysis between the 11-year average NPP and corresponding climate
21 variables was implemented on both regional and pixel scales. The Pearson product moment

1 correlation coefficient (R) was used to calculate the correlation between the NPP and annual
2 mean precipitation and annual mean temperature. A high R-value signifies a positive
3 relationship while a low R-value represents the opposite. A positive R implies that the NPP
4 has the same trend with temperature or precipitation, while a negative R implies the opposite.
5 Additionally, a zonal analysis was conducted to examine the NPP pattern along precipitation
6 and temperature gradients. Zonal analysis is one of the most important spatial analysis tools in
7 ArcGIS. It is the creation of an output raster (or statistics table) in which the desired function
8 is computed on the cell values from the input value raster that intersect or fall within each
9 zone of a specified input zone dataset (ESRI). The mean NPP value (dependent factor) for
10 each range of precipitation and temperature (independent factors) was calculated using
11 [Zonalstats] of ArcInfo, where the independent factors were used as zones and the dependent
12 factor was used as a value.

13

14 *2.5 Validation of MODIS data using flux tower data*

15

16 Eddy flux towers provide valuable opportunities to validate satellite data, because they
17 measure carbon, water and energy exchange on a long-term and continuous basis (Running *et*
18 *al.*, 1999). GPP derived from eddy flux measurements in Qianyanzhou, Jiangxi province, was
19 employed to validate MODIS GPP. Vegetation around the tower is mainly artificial forest with
20 the stand age around 30 years including, e.g., planted pine and Chinese fir (Ma *et al.*, 2010).
21 Eddy flux GPP on daily basis in 2006 were provided by Qianyanzhou Experimental Station.
22 Correspondingly, MODIS GPP data in 2006 were downloaded. To match the footprint, subsets

1 of 4×4 pixels around the tower were extracted. In accordance with MODIS GPP, which is an
2 8-day composite, 8-day summations of eddy flux GPP were created to make a correlation with
3 average of MODIS GPP subsets.

4 5 **3. Results**

6 7 *3.1 Characteristics of climate variables*

8
9 Spatially, hydrothermal gradients present zonal characteristics. It is evident that temperatures
10 in the south and east are higher than those in the north and west (Fig.3a&b). On the other
11 hand, precipitation featured a decreasing trend from southeast to northwest. The mean decadal
12 temperature gradually increased from 2000 to 2010 based on the Mann-Kendall analysis (Fig.
13 3c), which was in an agreement with the overall warming trend. Moreover, the annual
14 precipitation slightly decreased following a linear trend over the study years (Fig. 3d).

15 16 *3.2 Spatial-temporal pattern of NPP*

17
18 GPP from Eddy flux measurements in Qianyanzhou was used to validate MODIS GPP (Fig.
19 4). The result showed a good correlation between the two data sources ($r = 0.79$, $P < 0.0001$).
20 Vegetation production in the current study was characterized utilizing NPP value intervals,
21 which presented great spatial variability (Fig. 5a). For the entire study area, the average
22 production in the south and east is higher than that in the north and west. The area with the

1 highest production was located in the southern part of the Yunnan province, where the
2 dominant vegetation is composed of a broad-leaved evergreen forest. NPP of the broad-leaved
3 evergreen forest in the Fujian province is the second highest within the whole study region.
4 The **third** highest NPP was in the southeastern part of the Sichuan province. The broad-leaved
5 evergreen forests in the middle and northern parts of the study area presented relative low
6 NPP values. Among conifer forests, the highest values were found in the southern part of the
7 study region, followed by most of the Fujian province, the western region and some regions
8 of the Hunan and Jiangxi provinces. The lowest NPP values of conifer forests are present in
9 the northern part of the study region. In particular, as a type of a conifer forest, Chinese fir
10 exhibits a similar NPP pattern as coniferous forests in general, except that it has its highest
11 NPP value in the Fujian province in the eastern part of the study region, but lower values in
12 the southern, western, central and northern part of the study region. In general, in the potential
13 distribution area of Chinese fir plantations, broad-leaved evergreen forests have the highest
14 production (Fig. 5b). Compared to NPP of other coniferous **forests in the region**, the value of
15 Chinese fir is relatively low, $626 \text{ g C m}^{-2} \text{ yr}^{-1}$.

16

17 Temporally, from 2000 to 2010, the NPP values of Chinese fir showed a decreasing trend (Fig.
18 6). During the period of 11 years, the highest NPP occurred in 2002 and the lowest one in
19 2009. The difference between these two years was 100 g C , about 15% of the average NPP.

20

21 The results of the spatial-temporal changes of NPP were obtained from the temporal change
22 tendency analysis conducted for the study years (Fig. 7a). The results showed a great increase

1 in NPP in the Fujian province and in the northern part of the study region. Parts of Sichuan,
2 Guizhou and Yunnan provinces, areas near the margins of the study region, also had similar
3 tendencies. On the contrary, NPP in most regions of Hunan and Jiangxi provinces declined
4 over the study period. Overall, the main production area of Chinese fir had an evidently
5 decreasing productivity, while NPP around most of the margin area increased. In terms of
6 vegetation type, percentages of NPP decreases during the period of 11 years are presented in
7 Fig. 7b. Farmland and deciduous broad-leaved forest showed mostly increasing NPP values
8 during the study years, while coniferous and evergreen broad-leaved forests had areas with
9 both increasing and decreasing NPP, with the proportions of decreasing NPP equaling 50%
10 and 55%, respectively. Chinese fir showed an especially high NPP decrease, 66%.

11

12 *3.3 Relationship between NPP pattern and climate variables*

13

14 Representations of spatial patterns may be different when observed on different scales. In
15 order to comprehensively clarify the relationship between the NPP pattern and climatic factors,
16 an analysis was conducted at three levels: the entire study region, **zonal analysis** and pixel
17 scale. Regionally, both temperature and precipitation presented positive correlations with NPP
18 values, where the correlation for precipitation was significant and higher than that for
19 temperature (Fig. 8a, b). The relationship between the NPP pattern and climatic factors was
20 further examined through a correlation analysis between NPP of each pixel and climate
21 geographically corresponding to NPP. The yearly average NPP and corresponding yearly data
22 of climate variables were correlated to each other using the Pearson product moment

1 correlation. Correlation coefficients of NPP and annual mean precipitation are shown in Fig.
2 9a. High correlations between the two variables were found in the central and northern part of
3 the whole study region, while low or negative correlations were detected in most southern
4 regions. The correlation coefficients between NPP and annual mean temperature are shown in
5 Fig. 9b. The central areas of the study region presented high r values, especially Hunan,
6 Jiangxi and Chongqing provinces, whereas negative r values were found within the southern
7 margin of the study region. For comparison, in the central and eastern areas of Chinese fir,
8 NPP values were more strongly correlated to temperature than to precipitation. In the northern
9 part they exhibited higher correlations with precipitation than with temperature, and in the
10 southern part negative correlations with both temperature and precipitation.

11
12 Additionally, the analysis of the NPP pattern along each climatic factor was implemented
13 utilizing a zonal analysis. Especially, the NPP patterns of Chinese fir, coniferous forests and
14 broad-leaved forests along climate variables were analyzed and compared. For all three
15 vegetation types, NPP along precipitation exhibited a more complex pattern than along
16 temperature (Fig. 10). In terms of precipitation, the NPP values of Chinese fir present a
17 gradual increase with the precipitation above 1400 mm and below 1700 mm, with a sharp
18 decrease above 1700 mm, and the same pattern was found in coniferous and broad-leaved
19 forests (Fig. 10a, c, e). Along decreasing precipitation below 1400 mm, the productivity of
20 both coniferous and broad-leaved forests presented a similar pattern: decreasing NPP with
21 precipitation above 970 mm and a sudden increase above 1100 mm and then a gradual
22 decrease until 1400 mm. Such pattern is not obvious in Chinese fir, except that there is a

1 sudden change at the precipitation level of 1100 mm.

2

3 In terms of temperature (Fig. 10b, d, f), an increasing trend of NPP of Chinese fir is evident
4 from the turning point temperature of 15.5°C, with a short, relatively stable interval ranging
5 from 15.5 °C to 19 °C. A similar pattern was found in coniferous and broad-leaved forests,
6 with a small difference within the interval from 15.5 °C to 19 °C. Within this interval, the
7 NPP values of coniferous forests present a gradual increase, while broad-leaved forests
8 exhibit a sudden increase and then a slow decrease. In comparison, the pattern of NPP along
9 the annual average temperature experienced by Chinese fir is similar with that of coniferous
10 forests, both of which experience decreasing NPP values along the temperature until 15.5 °C
11 despite stronger NPP fluctuation in Chinese fir and a greater decrease in coniferous forests.
12 NPP along temperature presents a more complicated pattern in broad-leaved forests. First
13 there is an increase in NPP, followed by a sudden decrease right before the turning point of
14 about 15.5 °C.

15

16

17

18

19

20

21

22

4. Discussion

4.1 Spatial pattern of NPP and climatic conditions

We got a good correlation between MODIS GPP and GPP from eddy flux measurements ($r = 0.79$, $P < 0.0001$) that was similar to the correlation in another study using satellite data from China (Wang et.al, 2014). MODIS GPP can be used to estimate the GPP within a pixel (an area of 1 km^2 in current study), while eddy tower measures GPP over a footprint that changes according to the wind speed and wind direction in one year. Differences in the spatial scales of the two methods may lead to differences in the predicted GPP of the MODIS-GPP algorithm and eddy tower (Wang et.al, 2014).

To characterize the spatial pattern of temperature and precipitation, we chose ordinary kriging as an estimator to interpolate the station data. Ordinary kriging is a linear optimum interpolation method for regionalized single variable with the minimum variance of the estimation variance. A cross-validation was conducted to estimate the interpolation accuracy, which showed a high correlation coefficient of 0.92 between the original temperature data and predicted kriging value, and 0.85 for that of precipitation data. Moreover, we compared our climatic data with WorldClim data (<http://www.worldclim.org/>), which is a set of global climate layers (climate grids) with a spatial resolution of about 1 square kilometer, and found a very similar characteristic between the those two dataset.

1 Factors in the physical environment that the growth and development of plants are radiation,
2 temperature, water and nutrients (Atkinson and Porter 1996). Three of these four factors are
3 climatic. Previously, a site analysis between climatic variables and the growth of Chinese fir
4 has been conducted on a local scale (Chen, 1980a). It was concluded that in Hunan and
5 Guizhou provinces, within the central part of the current study area, temperature was most
6 strongly correlated with the growth of Chinese fir, while in the Anhui province, within the
7 northern part of the current study area, the most strongly affecting climate factor was
8 precipitation. These previous results were consistent with our findings based on a correlation
9 analysis on a pixel scale, which characterized the relationship between NPP and climate
10 variables in more detail (Fig 7a).

11
12 Generally, forest production is correlated with both precipitation and temperature. Greater
13 precipitation and higher temperatures are accompanied with a higher production, as shown in
14 our results where the production in the south and east was higher than that in the north and
15 west. Del Grosso (2008) pointed that precipitation was better correlated with NPP than
16 temperature. In our study, considering the whole study area, precipitation had a greater
17 correlation with NPP than did temperature on a regional scale (Fig. 8). However, pixel-based
18 correlation analyses between climate variables and NPP showed that the relationship had great
19 spatial variability: NPP values were more strongly correlated with temperature than
20 precipitation in the central and eastern part of the study region, while NPP exhibited a greater
21 correlation with precipitation than with temperature in the northern part (Fig. 9). These results
22 brought out the importance of the scale effect. In the zonal analysis, NPP values generally

1 increased along both increasing precipitation and temperature gradients. However, NPP
2 values along the precipitation gradient presented more variability, which indicated that the
3 effect of precipitation on production is more complicated. [Chen et al. \(2005\)](#) have suggested
4 that the yearly distribution of precipitation has a strong effect on the natural vegetation growth.
5 In the current study, NPP values tended to decrease when precipitation was more than 1700
6 mm (Fig. 10a, c, e). High amounts of precipitation occur in the southern region of the study
7 area, such as Guangdong and Guangxi provinces, where rainfall is distributed unevenly ([Chen,
8 1980a](#)), causing periods of ample water supply but also drought. This also explains why the
9 production in the southern part of the study site has a negative correlation with precipitation
10 based on the pixel level analysis. Additionally, plantations appear to be more sensitive to
11 precipitation variability. As the results indicated, Chinese fir has its highest production in the
12 eastern part of the study region, not in the southern part as the natural forest did, which is the
13 only difference in the spatial pattern between artificial and natural forests.

14

15 *4.2 Climate change and NPP*

16

17 [Liu \(2010\)](#) has conducted an analysis on spatiotemporal changes in the climate of China that
18 the average temperature has increased significantly at the rate of 0.2°C per decade over the
19 period of 1955 to 2000 in south-eastern China ([Liu et al., 2010](#)). Additionally, the average
20 growing season has shifted 4.6-5.5 days forward and the average end has been 1.8-3.7 days
21 prolonged, increasing the length of the growing season by 6.9-8.7 days ([Liu et al., 2010](#)). **For
22 our data, a similar trend of increasing temperatures was recorded for the period (2000-2010).**

1 Warming tends to accelerate flowering and prolong the photosynthetically active period
2 (Cleland *et al.*, 2006; Berninger, 1997). Moreover, the length of the growing season
3 influences the annual vegetation production, longer seasons favoring the accumulation of
4 organic matter. Consequently, the production of vegetation will probably increase along an
5 increasing temperature. However, in the current study, the analysis on the temporal tendencies
6 of NPP indicated variability among different vegetation types, of which only farmland and
7 deciduous broad-leaved forest showed an increase over most regions of the study area during
8 the period of 11 years. NPP values of Chinese fir decreased for most pixels in most areas of
9 the study region, especially in the central production areas of Hunan and Jiangxi provinces.
10 Unlike in natural forests, the growth of plantation forests is manipulated by human beings to
11 some extent. Opposite to crops, the NPP values of plantations showed the largest decreases
12 among all vegetation types. There are two possibilities accounting for such phenomenon. One
13 possible reason is man-made causes, such as **land use change or** inappropriate silvicultural
14 management which results in soil degradation that influences the growth of plantations (Ding
15 *et al.*, 1999; Yang *et al.*, 2000). **Fires, harvest, deforestation or other disturbances that change**
16 **the land-use could alter terrestrial net fluxes at regional and global scales. However, it is**
17 **extremely challenging to estimate the carbon balance change associated with land-use change**
18 **because of current lack of information on the amount and spatial pattern of deforestation (Piao**
19 ***et al.*, 2012; Houghton, 2007). However, most of the plantation in south China is collective**
20 **owned stand. Farmers has always been repeatedly planted Chinese fir on the same sites**
21 **without intercropping or periods of fallow (Bi *et al.*, 2007), which reduce the land-use change**
22 **impact.** The other reason could be changing climate. Trees have a higher maintenance cost.

1 [Kremer et al. \(1996\)](#) proposed that a high air temperature also increases the maintenance
2 respiration, leading to decreases in NPP. In this study, broad-leaved and broad-leaved
3 deciduous forests were found to exhibit different changes during the study years. NPP of
4 broad-leaved forests decreased considerably, while deciduous forests showed a strong
5 increase. Such a difference indicated that the maintenance respiration of broad-leaved forests
6 in winter has probably greatly increased due to warming temperature.

7

8 It is evident that the production of vegetation in the study region did not benefit from an
9 increasing temperature. Despite the potential effects of increasing maintenance respiration or
10 anthropogenic influence, factors related to climate change, for instance increasing variability
11 in rainfall, enhanced frequency of extreme weather events, such as cold waves, droughts and
12 floods ([IPCC, 2007](#)), can influence the production of vegetation. The central and southern
13 parts of our study region experienced several extreme weather events during the study years,
14 including droughts in autumn 2004, floods and hurricanes in 2007 and snowstorms in 2008.

15 **Our results (Fig.6) show that NPP of Chinese fir decreased in 2005, which was to some**
16 **extend influenced by autumn droughts in 2004. Floods and hurricanes in 2007 also**
17 **corresponded with a declined NPP value in 2007 compared to that in 2006. While snowstorms**
18 **in 2008 made the NPP value even lower than that in 2007.** These events could potentially
19 increase the variability in precipitation, which may further explain why the production of
20 plantations had the greatest decreases, if they were more sensitive than natural forests to
21 precipitation variability. Additionally, as the climate changes, extreme events are becoming
22 more frequent on average ([IPCC, 2007](#)), which would potentially influence plantation

1 production, as relatively simple plantation ecosystems are highly vulnerable (Hartley, 2002).
2 Consequently, the capacity of carbon sequestration by artificial plantations would be
3 threatened. However, since the forest area in China has been increasing strongly (Piao et al,
4 2012), growth stocks of Chinese forests are still increasing.

5

6 **5. Conclusions**

7

8 The current study aimed to characterize the spatial-temporal pattern of NPP and reveal how it
9 is related to climatic factors in the potential distribution area of Chinese fir. A series of spatial
10 analyses were implemented to characterize the spatial pattern of NPP and climate factors, and
11 to analyze the impact of those factors on NPP. Generally, the production of vegetation
12 increased with the increasing precipitation and temperature, presenting a consistent spatial
13 pattern. Both broad-leaved forests and natural coniferous forests had their overall highest
14 production in the southern region, where the mean precipitation is highest although most
15 variable. On the other hand, Chinese fir showed its highest NPP in the eastern region, which
16 revealed that it is more vulnerable to precipitation variability than natural forests.
17 Consequently, the increased frequency of extreme weather events occurring in southern China,
18 potentially resulting from global climate change, might influence the growth of tree
19 plantations. The results of the current study showing that NPP of Chinese fir decreased more
20 than that of other vegetation types during the study years could be a consequence of the
21 climate change. Thus, carbon sequestration of artificial plantations could be a matter of
22 concern. These findings are expected to assist when developing strategies for the sustainable

1 development of Chinese fir plantations.

2

3 ***Acknowledgements*** The research was supported by the National Key Basic Research Program
4 of China (No. 2012CB416901), Young Talent Team Program of the Institute of Mountain
5 Hazards and Environment (SDSQB-2012-01) and Chinese Academy of Sciences Visiting
6 Professorships for Senior International Scientists (2013T1Z0028). We are grateful to the
7 researchers in Qianyanzhou Experimental Station for providing the flux tower GPP data.

8

9

10

11

12

13

14

15

16

17

18

19

20

21

22

1 **References**

2

3 Atkinson, D., Porter, J., 1996. Temperature, plant development and crop yields. Trends Plant
4 Sci. 1, 119-124.

5

6 Bartholomé, E., Belward, A., 2005. GLC2000: a new approach to global land cover mapping
7 from Earth observation data. Inter. J. Remote Sens. 26, 1959-1977.

8

9 Berninger, F., 1997. Effects of drought and phenology on GPP in *Pinus sylvestris*: a
10 simulation study along a geographical gradient. Funct. Ecol. 11, 33-42.

11

12 Bi, J., Blanco, J. A., Seely, B., et al., 2007. Yield decline in Chinese-fir plantations: a
13 simulation investigation with implications for model complexity. Canadian Journal of Forest
14 Research 37(9), 1615-1630.

15

16 Bivand, R. Tim Keitt and Barry Rowlingson. "rgdal: Bindings for the Geospatial Data
17 Abstraction Library". R package version 0.8-16, 2014.

18

19 Bivand, R. Pebesma, E. Gomez-Rubio Z., Applied spatial data analysis with R, Second edition.
20 Springer, NY, 2013

21

22 Chen, C., Feng, Z., Dong, M., 1980a. Correlative analysis between the growth of

1 *Cunninghamia lanceolata* and climate factors. Ecological Studies on the Artificial
2 *Cunninghamia lanceolata* Forests 65-86.
3
4 Chen, C., Feng, Z., 1980b. Studies on the microclimate of the artificial *Cunninghamia*
5 *lanceolata* forests in Hui-Tong county of Hunan province. Ecological Studies on the Artificial
6 *Cunninghamia lanceolata* Forests 87-97.
7
8 Chen, Z., Wang, S., Wang, Y., Zhao, B., 2005. Degradation of Inner Mongolia grassland
9 ecosystem and management through fencing and ecological migrating. The Japan -Korea-
10 China Symposium on Grassland Agriculture and Animal Production 27-29.
11
12 Cleland, E., Chiariello, N., Loarie, S., Mooney, H., Field, C., 2006. Diverse responses of
13 phenology to global changes in a grassland ecosystem. PNAS 103, 13740-13744.
14
15 Data Sharing Network of Earth System Science. <http://www.geodata.cn>. 2012.
16
17 Del Grosso, S., Parton, W., Stohlgren, T., et al, 2008. Global potential net primary production
18 predicted from vegetation class, precipitation, and temperature. Ecology 89(8), 2117-2126.
19
20 Ding, Y., Tian, Y., Qi, L., 1999. A testing simulation with forecast on long-term productivity
21 of Chinese-fir plantations. Forestry Studies in China. 1, 34-38.
22

1 [ESRI. http://support.esri.com/en/knowledgebase/GISDictionary/term/zonal%20analysis](http://support.esri.com/en/knowledgebase/GISDictionary/term/zonal%20analysis)

2

3 Fang, J., Chen, A., Peng, C., Zhao, S., Ci, L., 2001. Changes in forest biomass carbon storage
4 in China between 1949 and 1998. *Science* 292, 2320-2322.

5

6 Fang, Q., 1987. Influence of continuous cropping on soil fertility and stand growth in
7 Chinese-fir plantations. *Sci. Silvae Sin.* 23, 389-397.

8

9 Field, C., Randerson, J., Malmstrom, C., 1995. Global net primary production: combining
10 ecology and remote sensing. *Remote Sen. Environ.* 51, 74-88.

11

12 Fung, I., Field, C., Berry, J., Thompson, M., Randerson, J., Malmström, C., Vitousek, P.,
13 Collatz, G., Sellers, P., Randall, D., Denning, A., Badeck, F., John, J., 1997. Carbon 13
14 exchanges between the atmosphere and biosphere. *Global Biogeochem. Cycles* 11, 507-533.

15

16 Hartley, M., 2002. Rationale and methods for conserving biodiversity in plantation forests.
17 *For. Ecol. Manage.* 155, 81-95.

18

19 [Houghton, R., 2007. Balancing the global carbon budget. *Annual Review of Earth and*
20 *Planetary Sciences* 35, 313-347.](#)

21

22 IGBP Terrestrial Carbon Working Group, 1998. The terrestrial carbon cycle: implications for

1 the Kyoto Protocol. Science 280, 1393-1394.

2

3 Kremer, R., Hunt, E., Running, S., Coughlan, J., 1996. Simulating vegetational and
4 hydrologic responses to natural climatic variation and GCM-predicted climate change in a
5 semi-arid ecosystem in Washington, U.S.A. J. Arid Environ. 33, 23-38.

6

7 Liu, B., Henderson, M., Zhang, Y., Xu, M., 2010. Spatiotemporal change in China's climatic
8 growing season: 1955-2000. Climatic Change 99, 93-118.

9

10 Lu, H., 1980. A discussion on wood structure of *Cunninghamia lanceolata* for different age
11 stages and relation between false ring and climatic factors. Ecological Studies on the Artificial
12 *Cunninghamia lanceolata* Forests 226-237.

13

14 Ma, X., 2001. Advance in researches on productivity decline of replanting Chinese-fir forests.
15 J. Fujian For. Coll. 21, 380-384.

16

17 Ma, Z., Wang, H., Wang, S., Li, Q., Wang, Y., Wang, H.Q., 2010. Impact of a severe ice storm
18 on subtropical plantations at Qianyanzhou, Jiangxi, China. Chin. J. Plant Ecol. 34, 204-212.

19

20 Melillo, J., McGuire, A., Kicklighter, D., Moore, III B., Vorosmarty, C., Schloss, A., 1993.
21 Global climate change and terrestrial net primary production. Nature 363, 234-240.

22

1 Monteith, J., 1972. Solar radiation and productivity in tropical ecosystems. *J. Appl. Ecol.* 9,
2 747-766.

3

4 Nemani, R., Keeling, C., Hashimoto, H., Jolly, W., Piper, S., Tucker, C., Myneni, R., Running,
5 S., 2003. Climate-driven increases in global terrestrial net primary production from 1982 to
6 1999. *Science* 300, 1560-1563.

7

8 Piao, S. L., Ito, A., Li, S. G., et al., 2012. The carbon budget of terrestrial ecosystems in East
9 Asia over the last two decades. *Biogeosciences* 9(9), 3571-3586.

10

11 Potter, C., Klooster, S., Myneni, R., Genovese, V., 2004. Terrestrial carbon sinks predicted
12 from MODIS satellite data and ecosystem modeling. *Earth Observer* 16, 15-20.

13

14 Prentice, I., Farquhar, G., Fasham, M., Goulden, M., Heimann, M., Jaramillo, V., Kheshgi, H.,
15 Le Que´re´, C., Scholes, R., Wallace, D., 2001. The carbon cycle and atmospheric carbon
16 dioxide, in *Climate Change 2001: The Scientific Basis-Contribution of Working Group I to*
17 *the Third Assessment Report of the Intergovernmental Panel on Climate Change*. Cambridge
18 University Press, New York, pp.182-237.

19

20 R Core Team. "R: A language and environment for statistical computing". R Foundation for
21 Statistical Computing, Vienna, Austria, 2014.

22

1 Ruimy, A., Dedieu, G., Saugier, B., 1994. Methodology for the estimation of terrestrial net
2 primary production from remotely sensed data. *J. Geophys. Res.* 99(D3), 5263-5284.
3
4 Running, S., Hunt, E., 1993. Generalization of a forest ecosystem process model for other
5 biomes, BIOME-BGC, and an application for global-scale models, in scaling physiological
6 processes: leaf to globe, Elsevier, New York, pp.141-158.
7
8 Running, S., Coughlan, J., 1988. A general model of forest ecosystem processes for regional
9 applications: I. Hydrologic balance, canopy gas exchange and primary production processes.
10 *Ecol. Modell.* 42, 125-154.
11
12 Running, S., Baldocchi, D., Turner, D., Gower, S., Bakwin, P., Hibbard, K., 1999. A global
13 terrestrial monitoring network integrating tower fluxes, flask sampling, ecosystem modeling
14 and EOS satellite data. *Remote Sens. Environ.* 70, 108-128.
15
16 Solomon, S., Qin, D., Manning, M., Chen, Z., Marquis, M., Averyt, K., Tignor, M., Miller, H.
17 (eds.), 2007. IPCC: Climate Change 2007: The Physical Science Basis. Contribution of
18 Working Group I to the Fourth Assessment Report of the Intergovernmental Panel on Climate
19 Change. Cambridge University Press, Cambridge, United Kingdom and New York, NY, USA.
20
21 Stow, D., Daeschner, S., Hope, A., Douglas, D., Petersen, A., Myneni, R., Zhou, L., Oechel,
22 W., 2003. Variability of the seasonally integrated normalized difference vegetation index

1 across the north slope of Alaska in the 1990s. *Inter. J. Remote Sens.* 24, 1111-1117.

2

3 United Nations Framework Convention on Climate Change, 1997. Kyoto Protocol to the

4 United Nations Framework Convention on Climate Change, UN, Geneva, 24.

5

6 Wang, Q., Wang, S., Zhang, J., 2009. Assessing the effects of vegetation types on carbon

7 storage fifteen years after reforestation on a Chinese fir site. *For. Ecol. Manage.* 258,

8 1437-1441.

9

10 Wang, L., Tian, B., Masoud, A., Koike, K., 2013. Relationship between remotely sensed

11 vegetation change and fracture zones induced by the 2008 Wenchuan earthquake, China. *J.*

12 *Earth Sci.* 24, 282-296.

13

14 Wang, X., Ma, M., Li, X., et.al, 2013. Validation of MODIS-GPP product at 10 flux sites in

15 northern China. *International Journal of Remote Sensing* 34(2), 587-599.

16

17 Wickham, H. *ggplot2: elegant graphics for data analysis.* Springer New York, 2009.

18

19 Wu, Z., 1984. *Chinese-fir.* China Forestry Publishing House. Beijing.

20

21 Yang, Y., Chen, G., Huang, B., 2000. Variation in the soil water and nutrients between

22 different rotation stands of Chinese-fir. *J. Nanjing For. Univ.* 24, 25-28.

1
2
3
4
5
6
7
8
9
10
11
12
13
14
15
16
17
18
19
20
21
22

Yue, S., Pilon, P., Cavadias, G, 2002. Power of the Mann-Kendall and Spearman's rho tests for detecting monotonic trends in hydrological series. *J. Hydrol.* 259, 254-271.

Zhang, Y., Xu, M., Chen, H., Adams J., 2009. Global pattern of NPP to GPP ratio derived from MODIS data: effects of ecosystem type, geographical location and climate. *Global Ecol. Biogeography.* 18, 280-290.

Zhao, M., Running, S., Nemani, R., 2006. Sensitivity of Moderate Resolution Imaging Spectroradiometer (MODIS) terrestrial primary production to the accuracy of meteorological reanalyses. *J. Geophysical Res.: Biogeosci.* 111(G1), 2005-2012.

Zhao, M., Heinsch, F., Nemani, R., Running, S., 2005. Improvements of the MODIS terrestrial gross and net primary production global dataset. *Remote Sens. Environ.* 95, 164-176.

Zhao, M., Running, S., 2010. Drought-induced reduction in global terrestrial net primary production from 2000 through 2009. *Science* 329, 940-943.

1 **Figure legends**

2 **Figure 1** Location of the study area (green) in southern China. Names and borders of
3 provinces are shown. Flags represent weather stations located within the study region. Red
4 asterisk indicates Huitong county, which is the central place of Chinese fir production.

5
6 **Figure 2** Distribution of eight vegetation classes as retrieved from the Global Landcover 2000
7 web site and Chinese artificial forest map.

8
9 **Figure 3** Spatial patterns and temporal changes of climate variables in the study region. (a)
10 temperature surface; (b) precipitation surface; (c) mean annual temperature (MAT); (d) mean
11 annual precipitation (MAP). Mean annual temperature shows significantly increasing trend
12 except a relatively low value in 2008, while mean annual precipitation shows significantly
13 decreasing trend during the study years.

14
15 **Figure 4** A linear comparison of MODIS GPP and observed gross primary production (g C
16 m⁻²·d⁻¹) at the eddy flux tower site in Qianyanzhou, Jiangxi province. MODIS data are
17 positively related to ground data ($r = 0.79$, $P < 0.0001$, $n = 25$).

18
19 **Figure 5** Spatial pattern of NPP in the study region. (a) spatial pattern of average NPP during
20 study years, the intervals was chosen based on the quartile of cumulative distribution of the
21 NPP; (b) the mean NPP of each vegetation type. Error bars represent standard deviation
22 within vegetation type. Abbreviations: N, coniferous forest; CF, Chinese fir; EB, evergreen

1 broad-leaved forest; DB, deciduous broad-leaved forest; B, bush; F, farmland; M, meadow.

2 **Figure 6** Temporal changes of the total net primary production of Chinese fir in the study
3 region from 2000 to 2010 exhibit a significant decreasing trend.

4

5 **Figure 7** Temporal pattern of NPP in the study region. (a) pixel-based NPP temporal change
6 trend from 2000 to 2010; (b) the percentage of areas showing a decrease in NPP for each
7 vegetation type. Abbreviations: N, coniferous forest; CF, Chinese fir; EB, evergreen
8 broad-leaved forest; DB, deciduous broad-leaved forest; B, brush; F, farmland; M, meadow.

9

10 **Figure 8** Correlation between net primary production of Chinese fir and climate variables
11 from 2000 to 2010 on a regional scale. (a) mean annual precipitation (MAP); (b) mean annual
12 temperature (MAT). They both show linear trends. NPP of Chinese fir is significantly
13 correlated to MAP but not to MAT.

14

15 **Figure 9** Pixel scale correlation coefficients between NPP and (a) annual mean precipitation
16 and; (b) annual mean temperature.

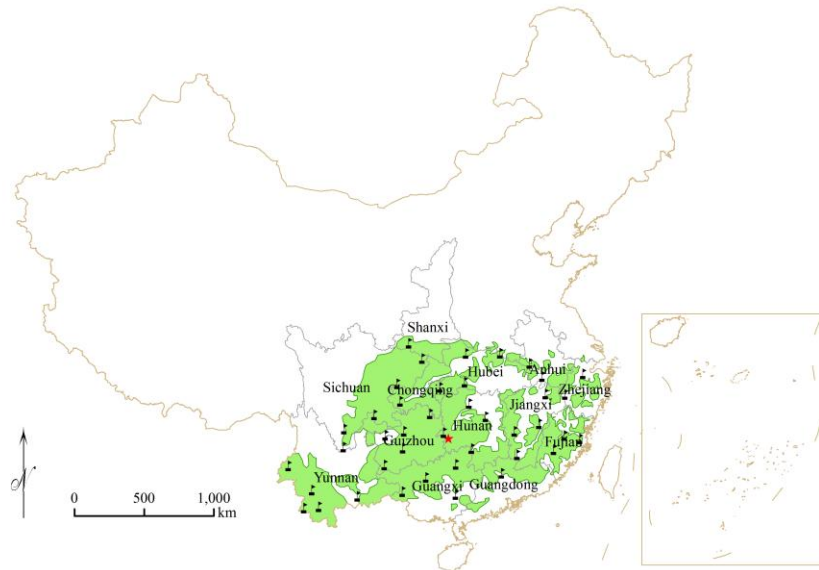
17

18 **Figure 10** Zonal analysis of the NPP pattern of (a) coniferous forest with precipitation; (b)
19 coniferous forest with temperature; (c) Chinese fir with precipitation; (d) Chinese fir with
20 temperature; (e) broad-leaved forest with precipitation; (f) broad-leaved forest with
21 temperature. Thin lines connect points representing the average NPP against precipitation or
22 temperature. Bold lines represent conditional averages.

23

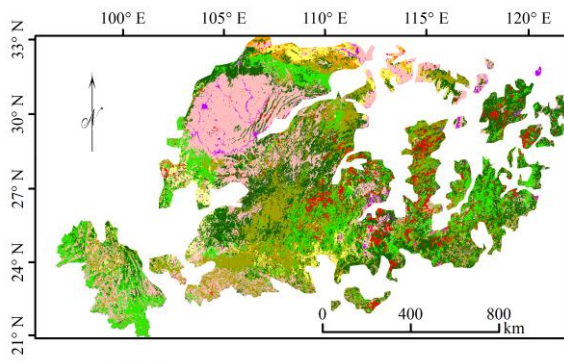
1 **Figure 1**

2
3
4
5
6
7
8
9
10
11
12
13
14
15
16
17
18
19
20
21
22
23



1 **Figure 2**

2
3
4
5
6
7
8
9
10
11
12
13
14
15
16
17
18
19
20
21
22
23

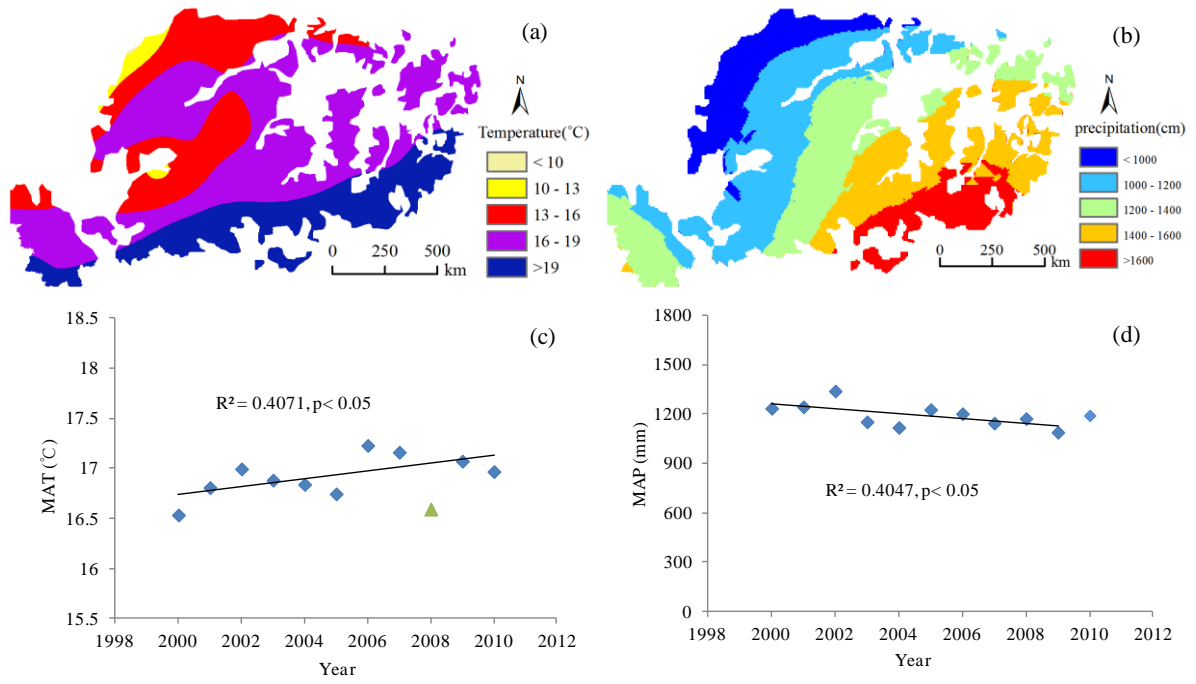


Legend

Chinese fir	Bush
Coniferous forest	Meadow
Broad-leaved evergreen forest	Farmland
Broad-leaved deciduous forest	Others

1 **Figure 3**

2
3
4
5
6
7
8
9
10
11
12
13
14
15
16
17
18
19
20
21
22



1 **Figure 4**

2

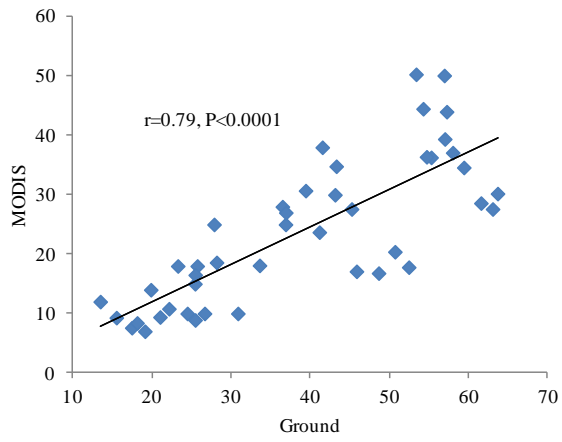
3

4

5

6

7



8

9

10

11

12

13

14

15

16

17

18

19

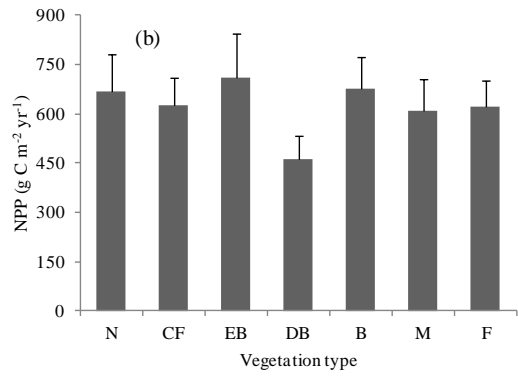
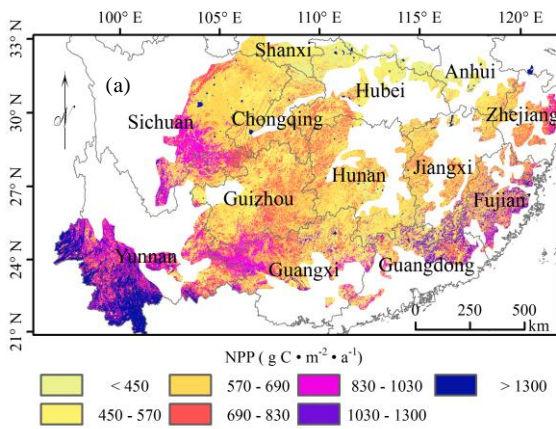
20

21

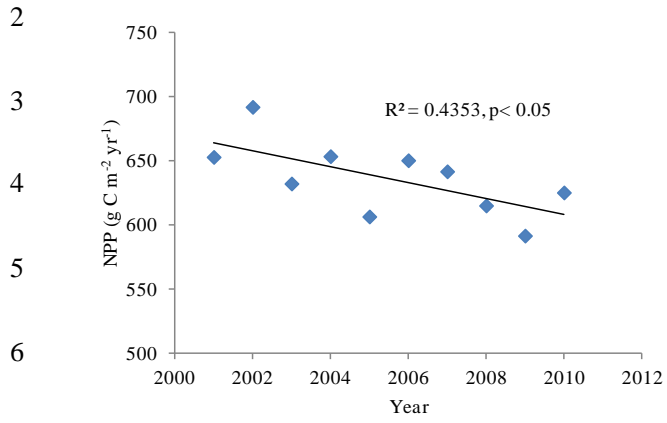
22

1 **Figure 5**

2
3
4
5
6
7
8
9
10
11
12
13
14
15
16
17
18
19
20
21
22
23



1 **Figure 6**



7

8

9

10

11

12

13

14

15

16

17

18

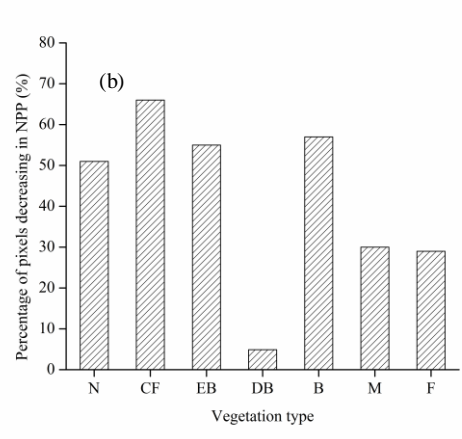
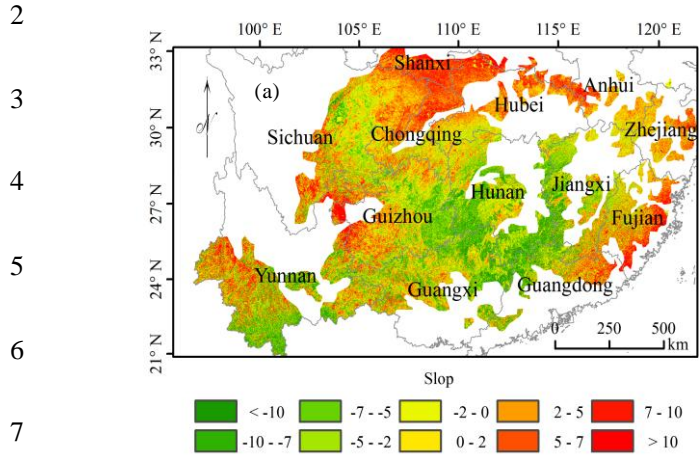
19

20

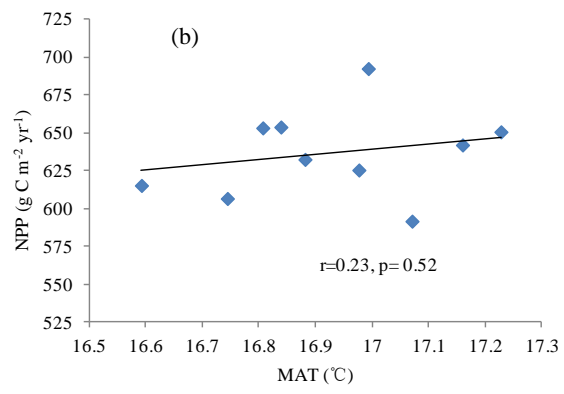
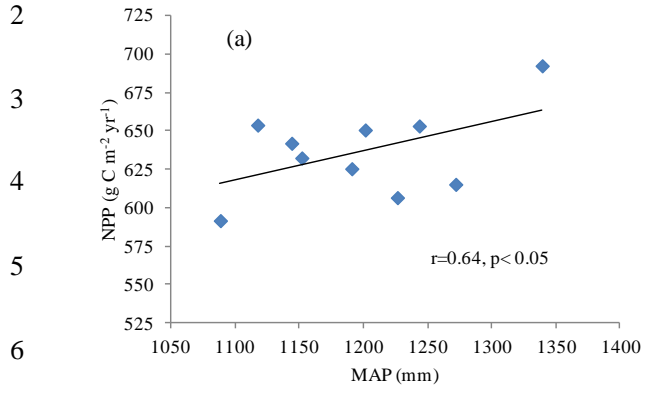
21

22

1 **Figure 7**

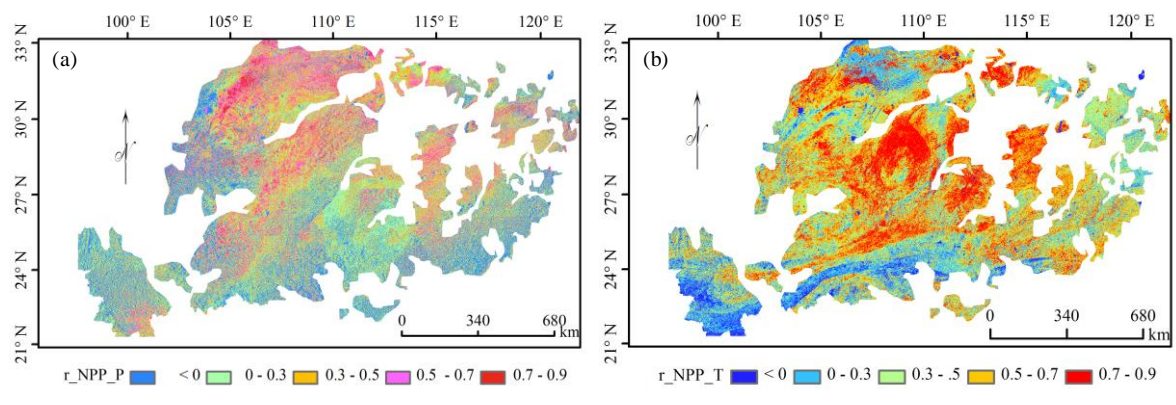


1 **Figure 8**



1 **Figure 9**

2
3
4
5
6
7
8
9
10
11
12
13
14
15
16
17
18
19
20
21
22



1 **Figure 10**

